Human Pathology (2020) **104**, 105−116

ELSEVIER

Human PATHOLOGY

www.elsevier.com/locate/humpath

Original contribution

Genetic basis of SMARCB1 protein loss in 22 sinonasal carcinomas☆,☆☆,☆☆☆

Snjezana Dogan MD[a,*], Paolo Cotzia MD[a], Ryan N. Ptashkin MS[a], Gouri J. Nanjangud PhD[b], Bin Xu MD, PhD[a], Amir Momeni Boroujeni MD[a], Marc A. Cohen MD[c], David G. Pfister MD[d], Manju L. Prasad MD, MBBS[e], Cristina R. Antonescu MD[a], Yingbei Chen MD, PhD[a], Mrinal M. Gounder MD[d,f]

[a] *Department of Pathology, Memorial Sloan Kettering Cancer Center, New York, NY, 10065, USA*
[b] *Molecular Cytogenetics, Core Facility, Memorial Sloan Kettering Cancer Center, New York, NY, 10065, USA*
[c] *Department of Surgery, Memorial Sloan Kettering Cancer Center, New York, NY, 10065, USA*
[d] *Department of Medicine, Memorial Sloan Kettering Cancer Center, 10065, USA*
[e] *Department of Pathology, Yale New Haven Hospital, New Haven, CT, 06520, USA*
[f] *Weill Cornell Medical College, New York, NY, 10065, USA*

Received 4 July 2020; accepted 11 August 2020

Available online 18 August 2020

Keywords:
Sinonasal SMARCB1-deficient carcinoma;
Homozygous deletion;
Next-generation sequencing

Abstract SMARCB1-deficient sinonasal carcinoma (SNC) is an aggressive malignancy characterized by INI1 loss mostly owing to homozygous *SMARCB1* deletion. With the exception of a few reported cases, these tumors have not been thoroughly studied by massive parallel sequencing (MPS). A retrospective cohort of 22 SMARCB1-deficient SNCs were studied by light microscopy, immunohistochemistry, fluorescence *in situ* hybridization (n = 9), targeted exome MPS (n = 12), and Fraction and Allele-Specific Copy Number Estimates from Tumor Sequencing (FACETS) (n = 10), a bioinformatics pipeline for copy number/zygosity assessment. SMARCB1-deficient SNC was found in 13 (59%) men and 9 (41%) women. Most common growth patterns were the basaloid pattern (59%), occurring mostly in men (77%), and plasmacytoid/eosinophilic/rhabdoid pattern (23%), arising mostly in women (80%). The former group was significantly younger (median age = 46 years, range = 24−54, vs 79 years, range = 66−95, $p < 0.0001$). Clear cell, pseudoglandular, glandular, spindle cell, and sarcomatoid features were variably present. SMARCB1-deficient SNC expressed cytokeratin (100%), p63 (72%), neuroendocrine markers (52%), CDX-2 (44%), S-100 (25%), CEA (4/4 cases), Hepatocyte (2/2 cases), and aberrant nuclear β-catenin (1/1 case). *SMARCB1* showed homozygous

☆ Competing interests: No competing financial interests exist for all contributory authors.
☆☆ Funding/Support: Research reported in this publication was supported by the Cancer Center Support Grant of the National Institutes of Health / National Cancer Institute under award number P30CA008748.
☆☆☆ Parts of the study were presented at USCAP 2018: Cotzia P, Ptashkin R, Gounder MM et al. Genetic and Histologic Spectrum of SMARCB1-deficient Carcinomas of the Head and Neck Including Sinonasal Tract, Thyroid and Skin. Lab Investigation. 2018; 98((suppl 1)):474−5.
* Corresponding author. Department of Pathology Memorial Sloan Kettering Cancer Center, 1275 York Avenue New York, New York, 10065, USA
E-mail address: dogans@mskcc.org (S. Dogan).

https://doi.org/10.1016/j.humpath.2020.08.004

deletion (68%), hemizygous deletion (16%), or truncating mutations associated with copy neutral loss of heterozygosity (11%). Coexisting genetic alterations were 22q loss including loss of *NF2* and *CHEK2* (50%), chromosome 7 gain (25%), and *TP53* V157F, *CDKN2A* W110*, and *CTNNB1* S45F mutations. At 2 years and 5 years, the disease-specific survival and disease-free survival were 70% and 35% and 13% and 0%, respectively. SMARCB1-deficient SNCs are phenotypically and genetically diverse, and these distinctions warrant further investigation for their biological and clinical significance.

1. Introduction

SMARCB1 gene, a putative tumor suppressor gene [1], is located at 22q11.2 and is a member of SWItch/sucrose nonfermentable (SWI/SNF) chromatin remodeling complex. SWI/SNF, ie, human analog BRG1/BRM-associated factor (BAF) complex, is a chromatin remodeling complex, which by modifying the spatial configuration of the DNA regulates the accessibility to gene transcription factors [2,3]. Somatic *SMARCB1* alterations, typically whole-gene deletion, were found in various malignancies including rhabdoid tumors [4], medulloblastoma [5], epithelioid sarcoma [6], medullary renal cell carcinoma [7], cribriform neuroepithelial tumor [8], and poorly differentiated chordoma [9] and, more recently, in a subset of aggressive sinonasal carcinomas (SNCs) [10–12]. SMARCB1-deficient SNC was first reported in 2014 [10–12] as an aggressive sinonasal malignancy characterized by SMARCB1 (INI1) protein loss and somatic *SMARCB1* gene deletion. Although most reported cases tend to display undifferentiated morphology reminiscent of sinonasal undifferentiated carcinoma, these tumors can be rather heterogeneous by their morphology and immunophenotype [13–15]. SMARCB1 protein loss could be explained by homozygous *SMARCB1* gene deletion detected by fluorescence *in situ* hybridization (FISH) in most cases [13]. However, the genome of SMARCB1-deficient SNC has not been studied in greater detail, and the current knowledge is limited to a few reported cases [10,16,17]. Here, we performed a detailed phenotypic and molecular characterization of our retrospective cohort of SMARCB1-deficient SNCs.

2. Materials and methods

2.1. Cases

The study was approved by the Internal Review Board of Memorial Sloan Kettering Cancer Center (MSKCC). Twenty-two cases of primary sinonasal SMARCB1-deficient carcinomas were retrieved from the MSKCC pathology archive, including 4 research and 18 clinical cases. All cases were reviewed by at least one pathologist with an interest in head and neck pathology (S.D.). Four cases were reported in the study by Dogan et al [16], and the outcome of 15 patients was included in another study [18].

2.2. DNA extraction and molecular testing

In 12 cases, targeted exome massive parallel sequencing (MPS) assay, MSK-Integrated Mutation Profiling of Actionable Cancer Targets (MSK-IMPACT™), was performed to evaluate genetic alterations in 279–468 cancer-related genes as previously described [19,20]. DNA was extracted from formalin-fixed paraffin-embedded (FFPE) tumor sections and from normal tissue. Matched normal FFPE tissue or normal blood was used for DNA extraction in 10 cases, and unmatched pooled normal DNA was used in 2 cases. Copy number aberrations (CNAs) were identified by comparing the sequence coverage of targeted regions in a tumor sample relative to a standard diploid normal sample. CNAs were expressed as the $\log_2$-transformed tumor/normal ratio, and a minimum of 2.0-fold change was required to consider gene amplification or deletion [19,20]. Fraction and Allele-Specific Copy Number Estimates from Tumor Sequencing (FACETS) analysis for copy number/zygosity assessment was performed in 10 cases, with available matched normal DNA as previously described [21]. Oncogenicity was determined based on OncoKB annotation in cBioPortal [22].

2.3. FISH for the *SMARCB1* gene

Nine cases were evaluated for *SMARCB1* gene copy number status by FISH assay using 4-μm FFPE tissue sections. In 4 cases, bacterial artificial chromosome probes, including telomeric *EWSR1* and 22q11 (control probes), were used to assess the *SMARCB1* gene copy number status. In the presence of both control signals, either telomeric *EWSR1* or 22q11, two *SMARCB1* copies indicated normal/intact *SMARCB1* gene status, one *SMARCB1* copy indicated hemizygous deletion, and the absence of both *SMARCB1* copies indicated homozygous deletion as previously described [12]. In 5 cases, tricolor FISH was

Table 1 Clinical summary of patients with SMARCB1-deficient sinonasal carcinoma.

Patients	N = 22	*p* value
Sex (n = 23)		
Men	13 (59%)	
Age (years), median (range)	47.5 (24−95)	0.033
Women	9 (41%)	
Age (years), median (range)	66 (35−83)	
Stage		
T stage		
T1	0	
T2−T3	3 (14%)	
T4	18 (82%)	
Unknown	1 (5%)	
N stage		
N0	16 (73%)	
N1−N2	5 (23%)	
Unknown	1 (5%)	
M stage		
M0	19 (86%)	
M1	2 (9%)	
Unknown	1 (5%)	
Clinical stage		
I	0	
II−III	2 (9%)	
IV	19 (86%)	
Unknown	1 (5%)	
Treatment (n = 18)		
SxCRT	7 (39%)	
CRT	5 (28%)	
SxRT	2 (11%)	
SxC	1 (6%)	
Sx	1 (6%)	
C	1 (6%)	
Unknown	1 (6%)	
Recurrence/metastasis (n = 18)		
All	14 (78%)	
Local	7 (39%)	
Regional	4 (22%)	
Distant	11 (61%)	

Abbreviations: Sx, surgery; C, chemotherapy; RT, radiation therapy.

performed as detailed in the study by Jia et al [23]. In one case, the material was insufficient to perform molecular or cytogenetic studies.

2.4. Immunohistochemistry and *in situ* hybridization

Immunohistochemistry (IHC) was performed on the Ventana Benchmark Ultra platform (Ventana Medical Systems Inc., Tucson, AZ, USA) using a streptavidin-biotin-peroxidase procedure (iView; Ventana) or on a Leica-Bond-3 automated stainer platform (Leica, Buffalo Grove, IL), using a secondary polymeric detection kit (Refine, Leica) and a heat-based antigen retrieval method with a high pH retrieval buffer as per the manufacturer's recommendations. SMARCB1 protein status was assessed using INI1 antibody (clone 25/BAF47; BD Biosciences, Franklin Lakes, NJ, USA) at 1:200 dilution. The details on other antibodies used for IHC and ISH probes are summarized in Table S1. Positive IHC labeling in >25% cells was considered *positive*, in 6−25% cells was considered *focally positive*, in <1−5% cells was considered *very focally/rare cells positive*.

2.5. Statistical analysis

Statistical analysis was performed using Fisher's exact test for nonparametric variables and Student's *t*-test for continuous variables. All tests performed were two tailed. P values <0.05 were considered significant. Survival analysis was performed using the log-rank test.

3. Results

3.1. Clinical outcome

Most patients were men (13/22, 59%), presenting at the median age of 47.5 years (range = 24−95), and were significantly younger than women (9/22, 41%), who presented at the median age of 66 years (range = 35−83; p = 0.033). Clinical characteristics for all patients are summarized in Table 1. Clinical follow-up was available for 18 patients, with the median of 22 months (range = 1−199 months). At 2 years, 3 years, and 5 years, the overall survival was 66%, 50%, and 33%; disease-specific survival was 70%, 54%, and 35%; and disease-free survival was 13%, 13%, and 0%, respectively.

3.2. Pathologic and molecular features

3.2.1. Morphology

SMARCB1-deficient SNCs were morphologically diverse showing most often a basaloid growth pattern (13/22, 59%), reminiscent of undifferentiated or nonkeratinizing squamous cell carcinoma, with the tumor cells arranged in compact sheets and nests (Fig. 1), and were seen in relatively younger patients (median age = 46 years [range = 24−54]) and mostly men (10/13, 77%). The second most common, plasmacytoid/eosinophilic/rhabdoid pattern was found in 5 (23%) patients, who were mostly women (4/5, 80%, p = 0.047) and significantly older that the former group (median age = 79 years, range = 66−95, p < 0.0001). Two of the latter cases showed focal glandular differentiation. Pseudoglandular/eosinophilic and pseudoglandular/spindle cell morphology was seen in the remaining 4 (18%) patients (median age = 61 years, range = 47−69). The amount of intervening stroma varied from scanty, which was seen in tumors with a basaloid growth pattern, to abundant and mucoid in cases with

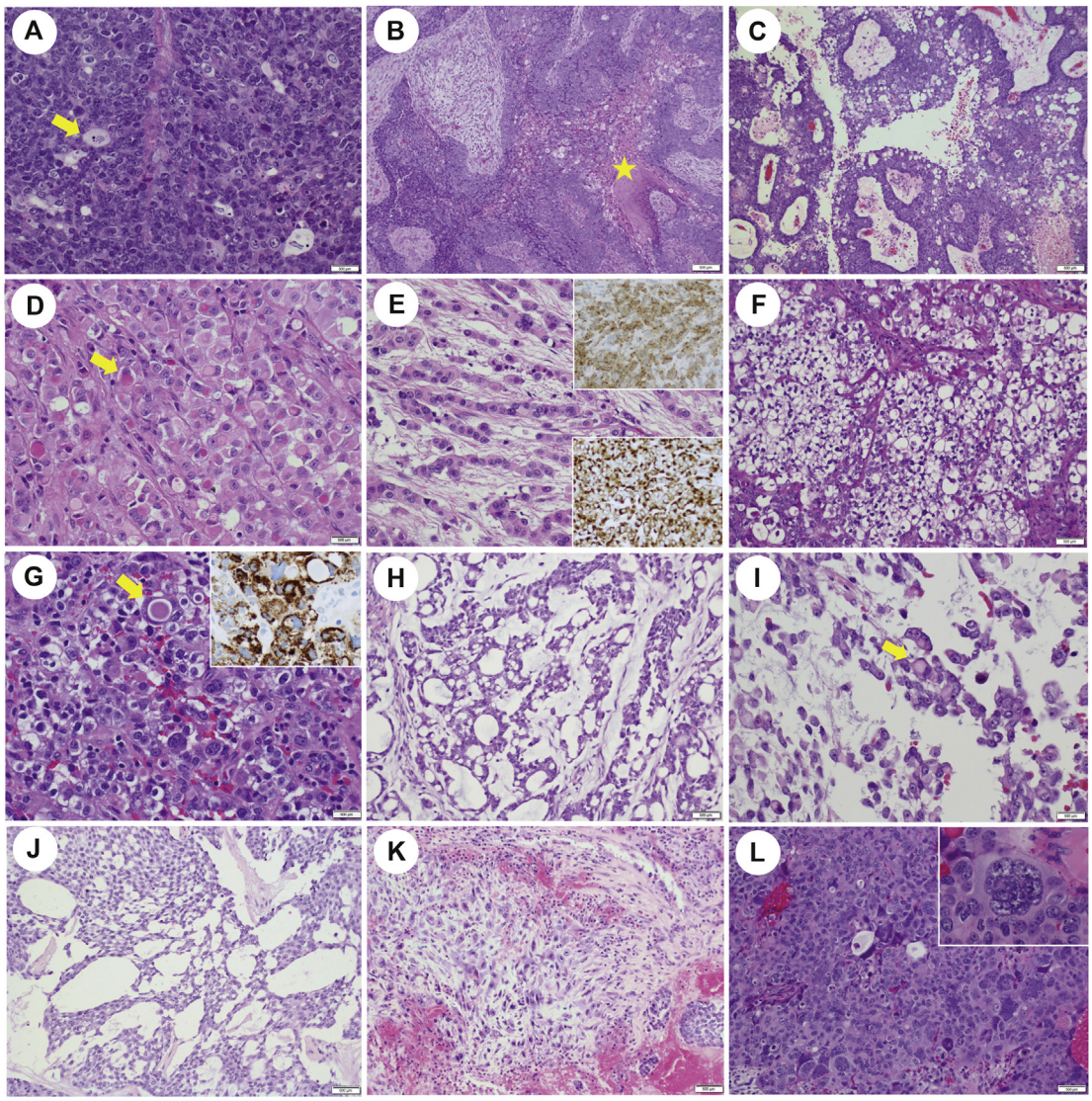

Fig. 1 Morphologic spectrum of SMARCB1-deficient SNCs. Basaloid growth pattern and scattered rhabdoid cells were subtle and showed clear cytoplasm with an eccentrically placed nucleus (yellow arrow; SN_62, A). Infiltrative growth with involvement of the surface epithelium (case SN_23, yellow star, B) and exophytic papillary features were seen (case SN_70, C). SN_26 comprised sheets (D) and trabeculae and cords (E) of oncocytic tumor cells with a striking predominance of rhabdoid cells; they were enlarged and contained deeply eosinophilic or red round cytoplasmic inclusions (yellow arrows, D) and showed diffuse and strong immunolabeling for synaptophysin (case SN_26, upper inset, E) and chromogranin (lower inset, E). SN_25 comprised sheets of predominantly clear cells interwoven with scanty fibrotic stroma (F) and scattered cells with large eosinophilic cytoplasmic inclusions (yellow arrow, G) and was strongly positive for Hepatocyte (inset, G). SN_24 comprised solid basaloid sheets of tumor cells (not shown) and pseudoglandular structures filled with basophilic mucoid material (H); discohesive single or small clusters of tumor cells were surrounded by abundant mucoid stroma. Rhabdoid cells are pointed by the yellow arrow (I). Areas with pseudoglandular appearance (J) alternated with sarcomatoid foci comprising pleomorphic sarcomatoid tumor cells were seen in SN_72 (K). Large bizarre multinucleated tumor cells were seen in SN_84 (yellow arrow, L). SNC, sinonasal carcinoma.

pseudoglandular, glandular and/or spindle cell features. Clear cell features, oncocytic, sarcomatoid foci and bizarre multinucleated giant cells were also variably present. The rhabdoid cells appearance ranged from subtle with clear cytoplasm and an eccentric nucleus to prominent with plasmacytoid appearance. Occasionally, increased amount of eosinophilic material formed large intracytoplasmic inclusions and, with peripherally located nuclei, provided a characteristic rhabdoid appearance (case SN_25), and some cases showed clear, *empty* cytoplasmic vacuoles (Fig. 1).

3.2.2. Mutation profile and SMARCB1 gene status

All cases (n = 22, 100%) tested either by the molecular or FISH method showed loss of at least one *SMARCB1* allele. Among the cases with available zygosity status (n = 19), most (13/19, 68%) showed homozygous

Table 2 Genetic characteristics of SMARCB1-deficient SNC.

Test	Case ID	Age/ sex	Histology	Gene	AA change	cDNA change	Variant class	Zygosity	OncoKB	Broad gains	Broad losses
MSK-IMPACT	SN_23	54/M	Basaloid and plasmacytoid/ eosinophilic	*SMARCB1*	n/a	n/a	Del	n/a	Likely onc		
				CDKN2A	A57V	c.170C > T	Missense	n/a	Unknown		
				INPP4A	Q550_L554del	c.1650_1664del	In-frame del	n/a	Unknown		
	SN_24	47/M	Pseudoglandular/ eosinophilic	*SMARCB1*	n/a	n/a	Del	Homozygous	Likely onc		
	SN_25	54/M	Basaloid, clear cell and plasmacytoid/ eosinophilic	*SMARCB1*	n/a	n/a	Del	Hemizygous	Likely onc		
				ETV6	R127W	n/a	Missense	Diploid	Unknown		
	SN_26	95/M	Plasmacytoid/ eosinophilic/ rhabdoid with a trabecular growth pattern	*SMARCB1*	n/a	n/a	Del	n/a	Likely onc	7	
				PDGFRA	I989T	c.2966T > C	Missense	n/a	Unknown		
				PTPRS	I962V	n/a	Missense	n/a	Unknown		
				ATR	X1913_splice	c.5739-3delACTTCCTT	Splice site	n/a	Unknown		
	SN_62	24/M	Basaloid	*SMARCB1*	n/a	n/a	Del	Hemizygous	Likely onc		
				CHEK2	n/a	n/a	Loss	Hemizygous	Unknown		
				MAPK1	n/a	n/a	Loss	Hemizygous	Unknown		
				NF2	n/a	n/a	Loss	Hemizygous	Unknown		
				TCF3	S359F	c.1076C > T	Missense	Diploid	Unknown		
				PTPRD	R123K	c.368G > A	Missense	Diploid	Unknown		
	SN_63	33/M	Basaloid	*SMARCB1*	n/a	n/a	Del	Homozygous	Likely onc	1q	
				MYCN	R383H	c.1148G > A	Missense	Diploid	Unknown		
				CHEK2	n/a	n/a	Loss	Hemizygous	Unknown		
				NF2	n/a	n/a	Loss	Hemizygous	Unknown		
	SN_74	43/M	Basaloid	*SMARCB1*	n/a	n/a	Del	Homozygous	Likely onc		
				BRCA2	Q1037K	c.3109C > A	Missense	Diploid	Unknown		
	SN_75	66F	Plasmacytoid/ eosinophilic/ rhabdoid with glandular features	*SMARCB1*	X265_splice	c.795 + 2_795 + 44del	Splice site	CN-LOH	Likely onc	7	2q35-36
				CHEK2	n/a	n/a	Loss	CN-LOH	Unknown		3q26-28
				CRKL	n/a	n/a	Loss	CN-LOH	Unknown		
				EP300	n/a	n/a	Loss	CN-LOH	Unknown		
				MAPK1	n/a	n/a	Loss	CN-LOH	Unknown		
				NF2	n/a	n/a	Loss	CN-LOH	Unknown		
				RAC2	n/a	n/a	Loss	CN-LOH	Unknown		
				PRKD1	X329_splice	c.986-2A > C	Splice site	Diploid	Unknown		
				MSH2	X314_splice	c.943-1G > A	Splice site	Diploid	Unknown		
				FH	A200V	c.599C > T	Missense	Diploid	Unknown		
MSK-IMPACT	SN_76	79F	Plasmacytoid/ eosinophilic/ rhabdoid with glandular features	*SMARCB1*	n/a	n/a	Deletion	Hemizygous	Likely onc	7	
				CHEK2	n/a	n/a	Loss	Hemizygous	Unknown		
				CRKL	n/a	n/a	Loss	Hemizygous	Unknown		
				EP300	n/a	n/a	Loss	Hemizygous	Unknown		
				MAPK1	n/a	n/a	Loss	Hemizygous	Unknown		

(*continued on next page*)

Table 2 (*continued*)

Test	Case ID	Age/ sex	Histology	Gene	AA change	cDNA change	Variant class	Zygosity	OncoKB	Broad gains	Broad losses
				NF2	n/a	n/a	Loss	Hemizygous	Unknown		
				RAC2	n/a	n/a	Loss	Hemizygous	Unknown		
				PREX2	A1284V	c.3851C > T	Missense	Diploid	Unknown		
				FUBP1	Intragenic del of exons 2-18	n/a	Intragenic del	n/a	Unknown		
	SN_78	53/F	Pseudoglandular/ spindle cells	*SMARCB1*	n/a	n/a	Del	Homozygous	Likely onc		
				CHEK2	n/a	n/a	Del	Homozygous	Likely onc		
				CRKL	n/a	n/a	Del	Homozygous	Unknown		
				MAPK1	n/a	n/a	Del	Homozygous	Unknown		
				NF2	n/a	n/a	Del	Homozygous	Likely onc		
				TP53	V157F	c.469G > T	Missense	Diploid	Likely onc		
				AR	R841H	c.2522G > A	Missense	Diploid	Unknown		
				WHSC1	V1287L	c.3859G > T	Missense	Diploid	Unknown		
	SN_81	26/M	Basaloid with clear cell features	*SMARCB1*	n/a	n/a	Deletion	Homozygous	Likely onc		
				CHEK2	n/a	n/a	Loss	Hemizygous	Unknown		
				CRKL	n/a	n/a	Deletion	Homozygous	Unknown		
				MAPK1	n/a	n/a	Deletion	Homozygous	Unknown		
				NF2	n/a	n/a	Loss	Hemizygous	Unknown		
	SN_85	51/F	Basaloid	*SMARCB1*	Y44*	c.132C > G	Nonsense	CN-LOH	Likely onc		
				CTTNB1	S45F	c.134C > T	Missense	n/a	Likely onc		
				*CDKN2AP14*ARF	G125R	c.373G > A	Missense	n/a	Unknown		
				CDKN2AP16INK4A	W110*	c.330G > A	Nonsense	n/a	Likely onc		
				RAD51D	R127W	c.379C > T	Missense	n/a	Unknown		
FISH	SN_70	35/F	Basaloid	*SMARCB1*	n/a	n/a	Del	Homozygous	n/a	n/a	n/a
	SN_71	76/F	Plasmacytoid/ eosinophilic/ rhabdoid					Hemizygous			
	SN_73	53/M	Basaloid					Homozygous			
	SN_77	37/F	Basaloid					Homozygous			
	SN_79	69/M	Pseudoglandular/ spindle cells					Homozygous			
	SN_84	48/M	Basaloid with multinucleated giant cells					Homozygous			
	SN_86	71/F	Pseudoglandular/ eosinophilic					Homozygous			
	SN_87	46/M	Basaloid					Homozygous			
	SN_88	83/F	Plasmacytoid/					Homozygous			

n/a	SN_72	53/M	eosinophilic/ rhabdoid Basaloid/spindle with sarcomatoid cells	n/a	n/a	n/a

Abbreviations: SNC, sinonasal carcinoma; AA, amino acid; del, deletion; onc, oncogenic; CN-LOH, copy neutral loss of heterozygosity; n/a, not available; MSK-IMPACT, MSK-Integrated Mutation Profiling of Actionable Cancer Targets; FISH, fluorescence *in situ* hybridization.

SMARCB1 deletion (Table 2 and Fig. 2). In 3 (16%) cases, there was hemizygous *SMARCB1* loss and no other *SMARCB1* mutation, 2 (11%) cases had a truncating mutation, *SMARCB1* X265_splice site or *SMARCB1* Y44∗, and each variant was associated with copy neutral loss of heterozygosity (CN-LOH; Fig. 3). In one case with hemizygous *SMARCB1* loss tested by FISH, the mutation status of the alternate allele remained unknown (Table 2). By MSK-IMPACT, 21 genes were mutated in 12 cases, with a median of 2 mutations per case (range = 0−5) excluding CNA. *SMARCB1* was the only gene with recurrent (likely) oncogenic alterations, and these often co-occurred with loss of the neighboring genes at 22q (6/12, 50%), including *NF2* and *CHEK2* in all such cases, and variable loss of *MAPK1, RAC2, CRKL*, and/or *EP300* (Table 2). Mutations in 3 other tumor suppressor genes, including a hot spot *CTNNB1* S45F, *TP53* V157F, and *CDKN2A* W110∗, were detected in 3 (25%) cases. Three (25%) cases showed chromosome 7 gain. Random broad copy alterations included 1q gain and 2q35-36 and 3q26-28 losses. No particular associations between the type of *SMARCB1* mutation, with or without concurrent alterations, and the tumor phenotype or outcome could be identified.

3.2.3. Immunophenotype

The immunohistochemical studies and *in situ* hybridization study results are summarized in Fig. 4. All cases were positive for at least one cytokeratin, with AE1/AE3 (19/19) and Cam5.2 (9/9) being the most reliable and consistently positive in all tested cases. The remaining 3 cases were positive either for CK7, CK20, and/or BerEP4. About 72% (13/18) of cases were positive for p63 and 59% (10/17) of cases were positive for p40. Weak/focal p63/p40 staining was observed in about one-third of cases showing nonbasaloid morphology. Among myoepithelial markers, S-100 was weakly/focally positive in 25% (5/20) cases, whereas calponin or smooth muscle actin expression was rare. Fifty-two percent (11/21) of cases were positive either for synaptophysin or chromogranin, including 2 cases with strong positive labeling, one of which was initially diagnosed as large cell neuroendocrine carcinoma (SN_26, Fig. 4) and both showing predominantly plasmacytoid/eosinophilic/rhabdoid morphology (Fig. 1). CDX-2 was expressed in 4 of 9 (44%) tested cases, CEA was expressed in 4 of 4 tested cases, and Hepatocyte was expressed in 2 of 2 tested cases including SN_25, where the liver metastasis was initially misdiagnosed as primary hepatocellular carcinoma. No case expressed NUT, and no high-risk human papillomavirus or Epstein-Barr virus was detected.

4. Discussion

In the present study, we further expanded the phenotypic spectrum of SMARCB1-deficient SNCs and found

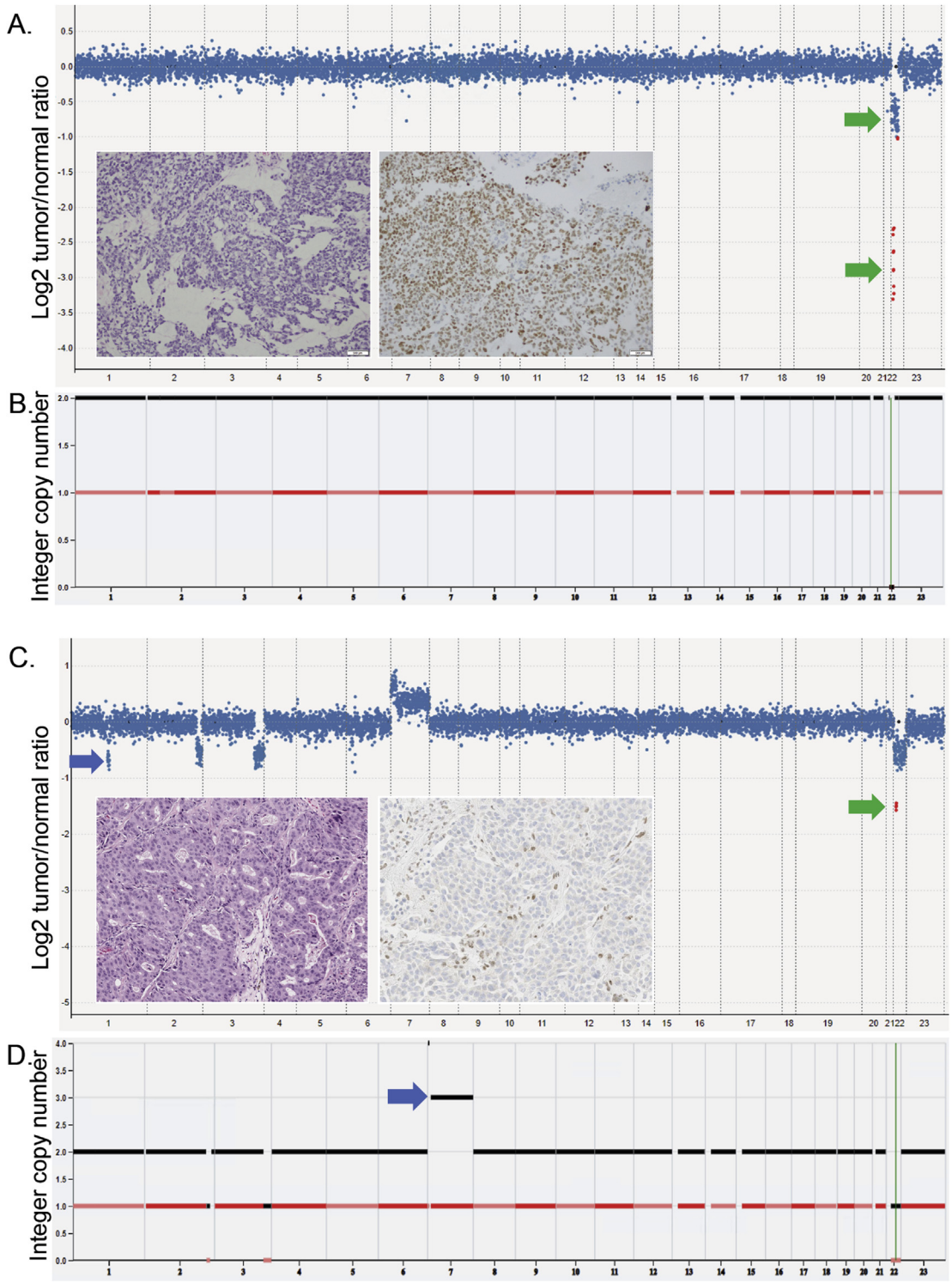

Fig. 2 *SMARCB1* deletion in SNC. Case SN_78 with predominantly pseudoglandular/spindle cell growth (left inset, H&E, A) was immunopositive for CDX-2 (right inset, A). The CNA plot depicts a homozygous deletion of the *SMARCB1* gene (lower green arrow) and deletion of the neighboring genes on 22q including *NF2* (upper green arrow). The y-axis depicts copy number changes expressed as the log2-transformed tumor/normal ratio as per their genomic positions indicated on the x-axis. Each dot represents one exon. Red dots indicate ≥2-fold tumor/normal ratio (A). FACETS analysis shows deletion of both *SMARCB1* alleles as indicated by the total integer copy number 0 (black line, y-axis). The red line indicates the minor allele. The vertical green line indicates the *SMARCB1* genomic position on chromosome 22 (B). Case SN_76 showed oncocytic gland-forming foci (left inset, H&E, C) and diffuse complete nuclear loss of SMARCB1 protein (right inset, Baf-47, C). The CNA plot shows *FUBP1* intragenic deletion (blue arrow), 2q35-36 and 3q26-28 losses, and hemizygous *SMARCB1* deletion (green arrow); FACETS indicated the total copy number of 1 (D). Heterozygous gain of chromosome 7 is indicated by total integer copy number 3 and minor allele copy number 1 (blue arrow, D). Abbreviations: CNA, copy number alteration; FACETS, Fraction and Allele-Specific Copy Number Estimates from Tumor Sequencing; H&E, hematoxylin and eosin; SNC, sinonasal carcinoma.

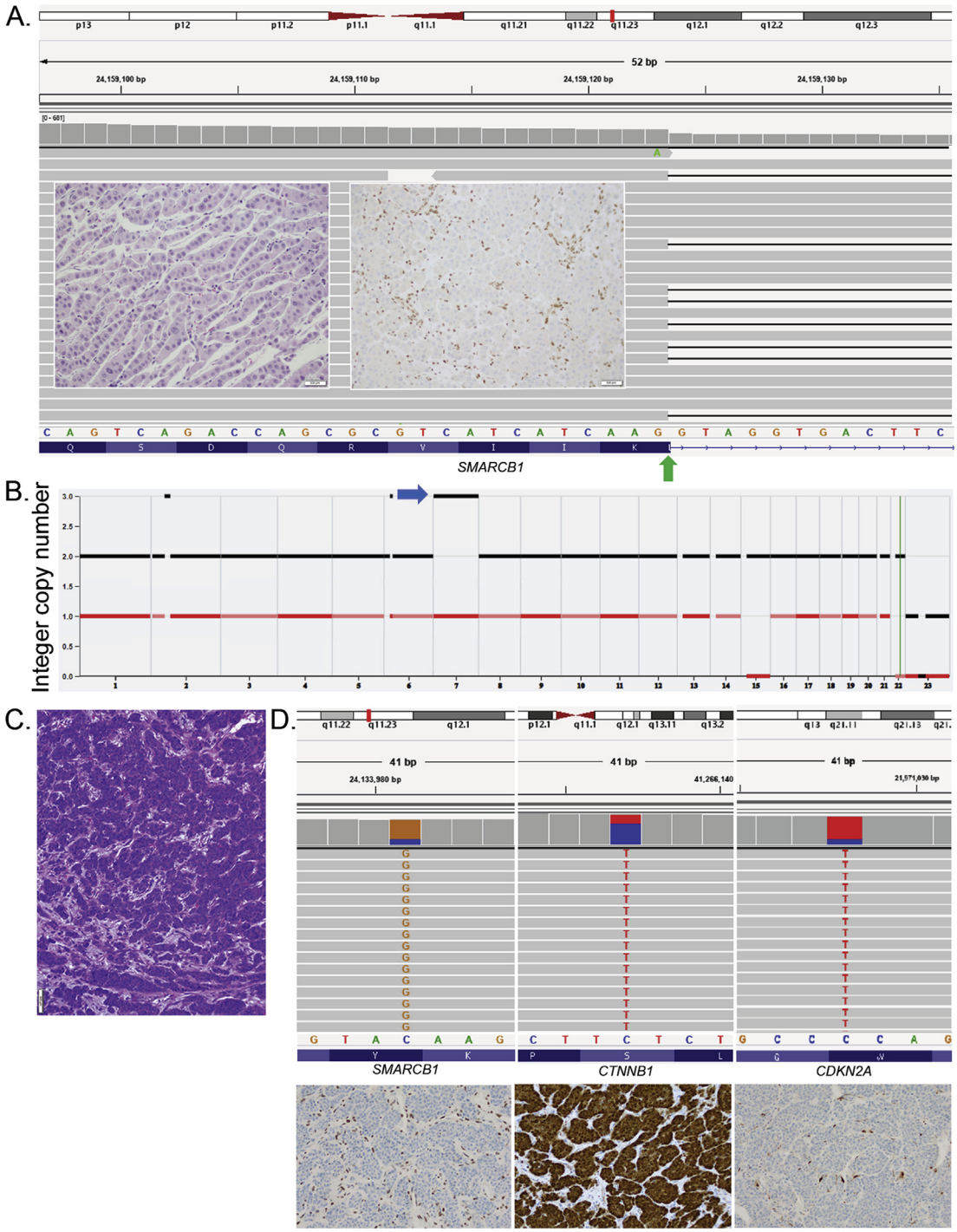

Fig. 3 Truncating *SMARCB1* mutations in SNC. In SN_75, oncocytic tumor cells formed cords and trabeculae (left inset, H&E, A). The IGV screenshot depicts *SMARCB1* splice site mutation c.795 + 2_795 + 44del, which results in a 44-bp deletion including the splice site (green arrow) as detected by MSK-IMPACT. Gray bars represent sequence reads that are aligned as per the reference genome at the bottom. Solid black lines represent sequence reads with *SMARCB1* mutation. Nitrogenous bases are color coded, and the corresponding amino acids are represented by blue rectangular bars. The noncoding sequence is shown as a blue line (A). Loss of nuclear Baf-47 in the tumor cells confirms the loss of normal SMARCB1 protein (right inset, A). CN-LOH detected by FACETS was consistent with the total *SMARCB1* copy number 2 (black) and minor allele copy number 0 (red). Heterozygous gain of chromosome 7 is indicated by the blue arrow (B). SN_85 showed a basaloid growth pattern (H&E, C) and harbored three oncogenic variants as depicted in IGV screenshots (D): *SMARCB1* Y44* (c.132C > G; upper left), *CTNNB1* S45F (c.134C > T; upper middle), and *CDKN2A* W110* (c.330G > A; upper right). Each mutation was consistent with the respective abnormal protein expression: nuclear loss of Baf-47 (lower left), aberrant nuclear expression of β-catenin (lower middle), and loss of p16 (lower right, D). Abbreviations: CNA, copy number alteration; FACETS, Fraction and Allele-Specific Copy Number Estimates from Tumor Sequencing; IGV, integrated genome viewer; bp, base pairs; CN-LOH, copy neutral loss of heterozygosity; SNC, sinonasal carcinoma; H&E, hematoxylin and eosin; MSK-IMPACT, MSK-Integrated Mutation Profiling of Actionable Cancer Targets.

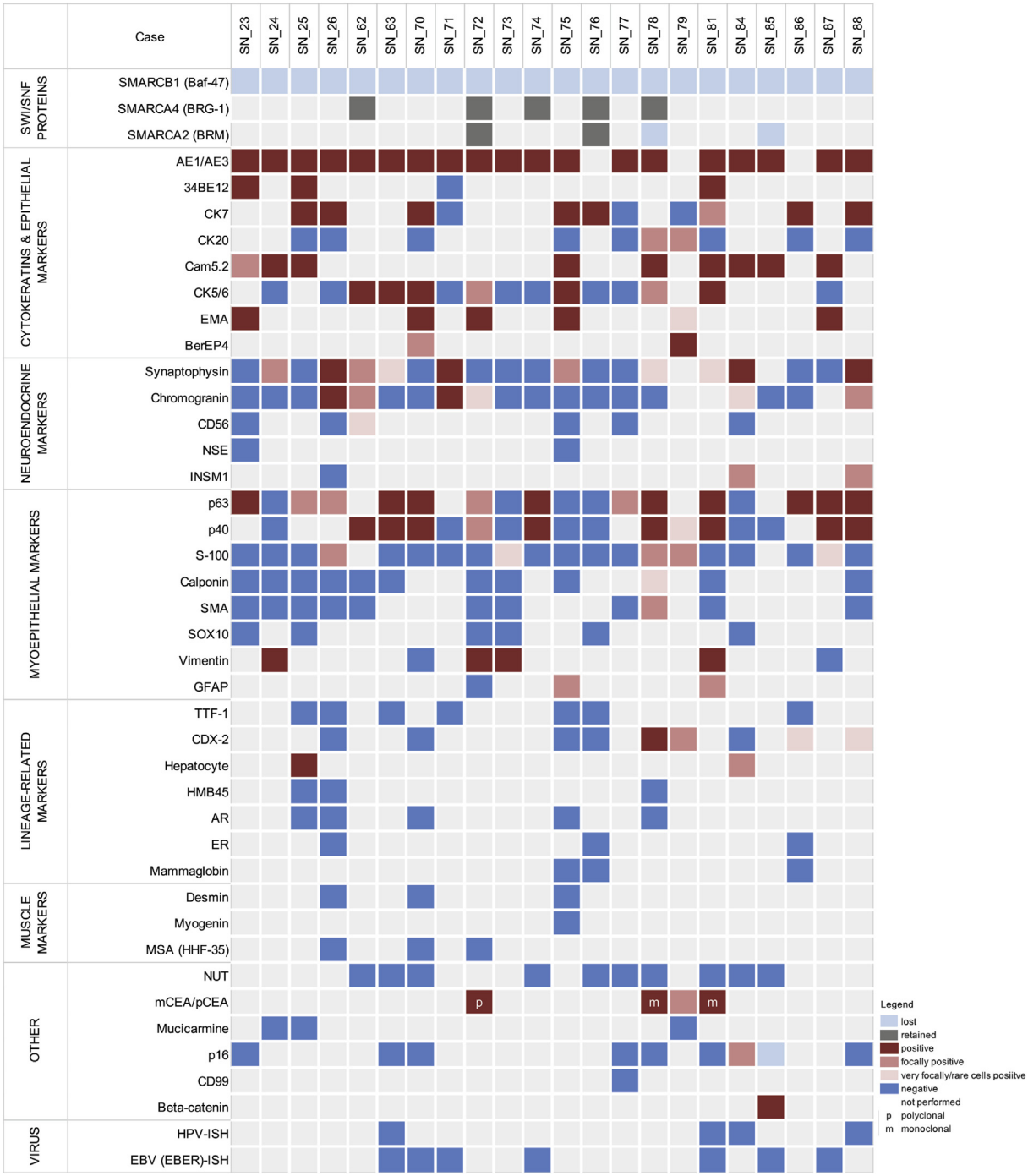

Fig. 4 Immunophenotype of SMARCB1-deficient SNC. Each column represents one case as indicated in the top row. The IHC results are color coded as per the legend. IHC, immunohistochemistry; SNC, sinonasal carcinoma; SWI/SNF, SWItch/sucrose nonfermentable; EBV, Epstein-Barr virus; HPV, human papillomavirus; ISH, *in situ* hybridization.

associations between the tumor morphology and patient characteristics. We provided a detailed molecular characterization of SMARCB1-deficient SNC, identified distinct genetic patterns consistent with SMARCB1 protein loss, and revealed coexisting, potentially significant genetic alterations.

After the description of first reported SMARCB1-deficient SNC cases in 2014, which were rather uniformly undifferentiated, multiple following studies demonstrated that these tumors can display a variety of histologies, suggesting that SMARCB1-deficient SNC might still be under-recognized and likely more common

than it has been currently perceived [13−15,24]. In line with the prior studies, our data further illustrate a wide morphological and immunophenotypic diversity of SMARCB1-deficient SNC. We have also found that the most common, basaloid growth pattern can be associated with relatively younger age and male sex, whereas carcinomas with plasmacytoid/eosinophilic/rhabdoid appearance might be more likely to arise in older women. In addition to the variety of morphologies, including pseudoglandular and glandular appearance reminiscent of high-grade adenocarcinoma, clear tumor cells, and spindle cell and sarcomatoid features, it is important to keep in mind that SMARCB1-deficient SNC can occasionally express immunomarkers commonly used to determine the site or organ of origin such as CDX-2 [15] and Hepatocyte. Therefore, caution must be exercised not to interpret poorly differentiated/high-grade CDX-2−positive carcinomas simply as sinonasal intestinal-type adenocarcinoma or as metastatic carcinoma of the lower gastrointestinal tract without further INI1 IHC workup. Similarly, a positive Hepatocyte immunostaining result should not be misinterpreted as metastatic hepatocellular carcinoma. INI1 IHC should not be either excluded from a diagnostic workup of high-grade SNC in the presence of a strong and diffuse neuroendocrine marker expression or aberrant nuclear β-catenin immunopositivity.

A very limited number of SMARCB1-deficient SNCs subjected to MPS published to date demonstrated *SMARCB1* whole-gene deletion in these cases [10,16,17]. FISH analysis showed homozygous deletion was the most predominant genetic alteration, followed by hemizygous deletion of *SMARCB1*. Rarely, *SMARCB1* was intact by FISH [13]. We confirmed homozygous *SMARCB1* deletion to be present in the majority of cases. Inactivating *SMARCB1* mutation coupled with CN-LOH could explain INI1 protein loss in a minor subset of cases. However, in some cases, hemizygous *SMARCB1* deletion was the only detected event, raising a question if INI1 protein loss in such cases could be partly due to gene rearrangement involving the alternate allele akin to that seen in medullary renal cell carcinomas [23] or due to microRNA-mediated epigenetic silencing of *SMARCB1* protein expression as reported in epithelioid sarcomas [25,26].

A paucity of coexisting (likely) oncogenic mutations including *CTNNB1*, *TP53*, and *CDKN2A* supportsthe role of deficient *SMARCB1* as a putative driver of malignant transformation in this subset of SNCs. However, a substantial degree of molecular heterogeneity is evident at the genetic level as half of the cases showed concurrent losses of the neighboring genes at 22q, including *NF2* and *CHEK2* losses. Recent methylation-based studies on atypical teratoid/rhabdoid tumors (AT/RT) helped substratify these tumors into three distinct, biologically relevant categories; although the AT/RT-MYC subset was enriched for focal *SMARCB1* gene deletions, AT/RT-TYR tumors comprised mostly cases with broad 22q deletions [27]. Therefore, larger, more comprehensive studies on SMARCB1-deficient SNC to explore the significance of concurrent, broad genetic losses at 22q would be justified.

Clinically, SMARCB1-deficient SNC has been shown to be aggressive malignancy with frequent recurrences and poor outcomes [13,18]. Our cohort, which originates from a single institution, supports the published data and demonstrates the aggressive nature of this sinonasal malignancy. Indeed, in the majority of patients with SMARCB1-deficient SNC, the disease is likely to recur within 2 years, and overall, less than one-third of patients will survive for 5 years.

The limitations of our study are mainly related to the lack of adequate tissues to perform further studies, for instance, to explore additional mechanisms of SMARCB1 protein loss in cases with hemizygous *SMARCB1* deletion. However, we have shown these cancers are phenotypically diverse, and less common morphologies such as the plasmacytoid/eosinophilic/rhabdoid pattern may be relatively more common in elderly female patients. We have demonstrated that SMARCB1-deficient SNCs display heterogeneity at the molecular level and that loss of SMARCB1 protein could be due to truncating mutations associated with CN-LOH in a significant minority of cases. Coexisting genetic alterations including recurrent *NF2* and *CHEK2* losses and chromosome 7 gain can provide the rationale for further, larger studies aiming to elucidate the biological significance of distinct molecular findings in SMARCB1-deficient SNC.

Appendix A Supplementary data

Supplementary data to this article can be found online at https://doi.org/10.1016/j.humpath.2020.08.004.

Acknowledgments

Research reported in this publication was supported by the Cancer Center Support Grant of the National Institutes of Health / National Cancer Institute under award number P30CA008748. S.D. and PC designed the research study; S.D., P.C., R.N.P., and G.J.N. performed research; M.A.C., D.G.P., and M.M.G. provided essential data of patients; G.N. and C.R.A. provided essential reagents and tools; S.D., P.C., R.N.P., G.J.N., B.X., A.M.B., M.L.P., C.R.A., and Y.C. analyzed the data; S.D., G.J.N., and B.X. wrote the manuscript; all authors were involved in critical review of the manuscript for important intellectual content.

References

[1] Biegel JA, Zhou J-Y, Rorke LB, Stenstrom C, Wainwright LM, Fogelgren B. Germ-line and acquired mutations of INI1 in atypical teratoid and rhabdoid tumors. Cancer Res 1999;59:74−9.

[2] Zhao K, Wang W, Rando OJ, Xue Y, Swiderek K, Kuo A, et al. Rapid and phosphoinositol-dependent binding of the SWI/SNF-like BAF complex to chromatin after T lymphocyte receptor signaling. Cell 1998;95:625–36.
[3] Clapier CR, Cairns BR. The biology of chromatin remodeling complexes. Annu Rev Biochem 2009;78:273–304.
[4] Versteege I, Sevenet N, Lange J, Rousseau-Merck M-F, Ambros P, Handgretinger R, et al. Truncating mutations of hSNF5/INI1 in aggressive paediatric cancer. Nature 1998;394:203.
[5] Biegel JA, Fogelgren B, Zhou J-Y, James CD, Janss AJ, Allen JC, et al. Mutations of the INI1 rhabdoid tumor suppressor gene in medulloblastomas and primitive neuroectodermal tumors of the central nervous system. Clin Canc Res 2000;6:2759–63.
[6] Modena P, Lualdi E, Facchinetti F, Galli L, Teixeira MR, Pilotti S, et al. SMARCB1/INI1 tumor suppressor gene is frequently inactivated in epithelioid sarcomas. Cancer Res 2005;65:4012–9.
[7] Cheng JX, Tretiakova M, Gong C, Mandal S, Krausz T, Taxy JB. Renal medullary carcinoma: rhabdoid features and the absence of INI1 expression as markers of aggressive behavior. Mod Pathol 2008;21:647.
[8] Hasselblatt M, Oyen F, Gesk S, Kordes U, Wrede B, Bergmann M, et al. Cribriform neuroepithelial tumor (CRINET): a nonrhabdoid ventricular tumor with INI1 loss and relatively favorable prognosis. J Neuropathol Exp Neurol 2009;68:1249–55.
[9] Mobley BC, McKenney JK, Bangs CD, Callahan K, Yeom KW, Schneppenheim R, et al. Loss of SMARCB1/INI1 expression in poorly differentiated chordomas. Acta Neuropathol 2010;120:745–53.
[10] Jamshidi F, Pleasance E, Li Y, Shen Y, Kasaian K, Corbett R, et al. Diagnostic value of next-generation sequencing in an unusual sphenoid tumor. Oncol 2014;19:623–30.
[11] Agaimy A, Koch M, Lell M, Semrau S, Dudek W, Wachter DL, et al. SMARCB1(INI1)-deficient sinonasal basaloid carcinoma: a novel member of the expanding family of SMARCB1-deficient neoplasms. Am J Surg Pathol 2014;38:1274–81.
[12] Bishop JA, Antonescu CR, Westra WH. SMARCB1 (INI-1)-deficient carcinomas of the sinonasal tract. Am J Surg Pathol 2014;38:1282–9.
[13] Agaimy A, Hartmann A, Antonescu CR, Chiosea SI, El-Mofty SK, Geddert H, et al. SMARCB1 (INI-1)-deficient sinonasal carcinoma: a series of 39 cases expanding the morphologic and clinicopathologic spectrum of a recently described entity. Am J Surg Pathol 2017;41:458–71.
[14] Kakkar A, Antony VM, Pramanik R, Sakthivel P, Singh CA, Jain D. SMARCB1 (INI1)–deficient sinonasal carcinoma: a series of 13 cases with assessment of histologic patterns. Hum Pathol 2019;83:59–67.
[15] Shah AA, Jain D, Ababneh E, Agaimy A, Hoschar AP, Griffith CC, et al. SMARCB1 (INI-1)-Deficient adenocarcinoma of the sinonasal tract: a potentially under-recognized form of sinonasal adenocarcinoma with occasional yolk sac tumor-like features. Head Neck Pathol 2019:1–8.
[16] Dogan S, Chute DJ, Xu B, Ptashkin RN, Chandramohan R, Casanova-Murphy J, et al. Frequent IDH2 R172 mutations in undifferentiated and poorly-differentiated sinonasal carcinomas. J Pathol 2017;242:400–8.
[17] Gomez-Acevedo H, Patterson JD, Sardar S, Gokden M, Das BC, Ussery DW, et al. SMARC-B1 deficient sinonasal carcinoma metastasis to the brain with next generation sequencing data: a case report of perineural invasion progressing to leptomeningeal invasion. BMC Canc 2019;19:827.
[18] Dogan S, Vasudevaraja V, Xu B, Serrano J, Ptashkin RN, Jung HJ, et al. DNA methylation-based classification of sinonasal undifferentiated carcinoma. Mod Pathol 2019;32:1447–59.
[19] Cheng DT, Mitchell TN, Zehir A, Shah RH, Benayed R, Syed A, et al. Memorial sloan kettering-integrated mutation profiling of actionable cancer Targets (MSK-IMPACT): a hybridization capture-based next-generation sequencing clinical assay for solid tumor molecular oncology. J Mol Diagn 2015;17:251–64.
[20] Zehir A, Benayed R, Shah RH, Syed A, Middha S, Kim HR, et al. Mutational landscape of metastatic cancer revealed from prospective clinical sequencing of 10,000 patients. Nat Med 2017;23:703.
[21] Shen R, Seshan VE. FACETS: allele-specific copy number and clonal heterogeneity analysis tool for high-throughput DNA sequencing. Nucleic Acids Res 2016;44:e131.
[22] Chakravarty D, Gao J, Phillips SM, Kundra R, Zhang H, Wang J, et al. OncoKB: a precision oncology knowledge base. JCO Precis Oncol 2017;2017:1–16.
[23] Jia L, Carlo MI, Khan H, Nanjangud GJ, Rana S, Cimera R, et al. Distinctive mechanisms underlie the loss of SMARCB1 protein expression in renal medullary carcinoma: morphologic and molecular analysis of 20 cases. Mod Pathol 2019;32:1329–43.
[24] Rooper LM, Bishop JA, Westra WH. INSM1 is a sensitive and specific marker of neuroendocrine differentiation in head and neck tumors. Am J Surg Pathol 2018;42:665–71.
[25] Papp G, Krausz T, Stricker TP, Szendrői M, Sápi Z. SMARCB1 expression in epithelioid sarcoma is regulated by miR-206, miR-381, and miR-671-5p on Both mRNA and protein levels. Genes Chromosomes Cancer 2014;53:168–76.
[26] Sapi Z, Papp G, Szendroi M, Papai Z, Plotar V, Krausz T, et al. Epigenetic regulation of SMARCB1 By miR-206,-381 and-671-5p is evident in a variety of SMARCB1 immunonegative soft tissue sarcomas, while miR-765 appears specific for epithelioid sarcoma. A miRNA study of 223 soft tissue sarcomas. Genes Chromosomes Cancer 2016;55:786–802.
[27] Johann PD, Erkek S, Zapatka M, Kerl K, Buchhalter I, Hovestadt V, et al. Atypical teratoid/rhabdoid tumors are comprised of three epigenetic subgroups with distinct enhancer landscapes. Canc Cell 2016;29:379–93.